Journal of Green Engineering (JGE)

Volume-10, Issue-12, December 2020

Design and Development of a Scatterometer to Detect Shallowly Buried Objects Using Microwaves at X-Band Frequency

[1]Patri Upender and [2]Anil Kumar

[1]*Research Scholar, Dept. of Electronics and Communication Engineering, Sri Satya Sai University of Technology & Medical Sciences, Sehore, Bhopal-Indore Road, MadhyaPradesh, India.*
[2]*Research Guide, Dept. of Electronics and Communication Engineering, Sri Satya Sai University of Technology & Medical Sciences, Sehore, Bhopal Indore Road,Madhya Pradesh, India.*

Abstract

This paper is intended to detect any sort of object, including non-metallic objects buried under the earth, by means of a radar device. In the military, this sort of device can be used to detect explosives hidden under the earth. For this reason, ground penetrating radar (GPR) is used. The technique used to image the subsurface using radar pulses is GPR. This approach uses electromagnetic waves from microwave bands. The object embedded under the surface of the ground is detected within the X-band frequency spectrum (8-12GHz). Radar is intended for a project in which the horn antenna is known to be an antenna that transmits and receives. Depending on the dielectric properties, various types of artifacts such as aluminum sheet, plastic sheet, glass plate, etc. have also been observed. Images are generated using MATLAB using these dispersing matrices. For signal processing, the A-scan and B- scan techniques are used. The aim of this paper is to explore the variations of GPR signals for various objects. Results shows clear discrimination between soil and the object buried.

Keywords: GPR, Microwaves, Soil moisture, X-Band, Radar, MATLAB.

Journal of Green Engineering, Vol. 10_12, 12988-13004.

Alpha Publishers

1 Introduction

Microwaves are defined as wavelengths between one metre to one millimetre and frequencies between 0.3GHz and 300GHz. At 8-12GHz(X-band) [1], experimental measurements are taken. When doing this experiment, the first question arises as to what should be the x and y distances at which the antenna should be held at various angles of incident[2]. Azimuth and elevation angles are necessary in order to calculate x and y distances. Azimuth and elevation angles are found by performing the antenna's experimental radiation pattern. In the anechoic chamber[3], the antenna pattern of the horn antenna used was calculated by taking E plane and H plane observations. When used in scatterometers at a certain height and at a certain distance from the ground, the antenna swath is defined as the total area covered by the face of the antenna. The buried object detection schematic is illustrated in Figure 1.

2 Basic Block Diagram

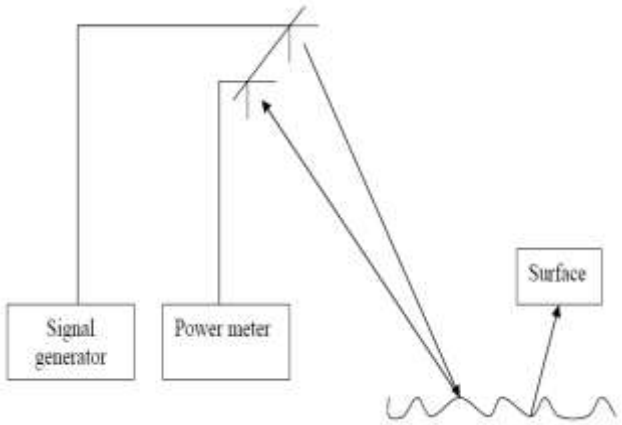

Figure 1 Schematic of the Setup for Detection of Buried Object

The frequency of the signals we use is high X-band frequencies (8-12GHz). The microwave klystron power supply is used to produce the signals in this band[4]. The power from the power supply of the klystron is fed to the antennas we are using in the process. A horn antenna is usually preferred. Such signals are transmitted to the ground and are then reflected by the earth. The receptor captures the reflected signal. It records the received power. There is now an entity hidden under the earth. This signal is transmitted again, penetrates into the ground and is mirrored by the object that absorbs the reflected signals by the receiving antenna that records this power. The power and these powers obtained above are compared and this will let us know the object type under the round. [5, 6].

Microwave radar imaging examinations and remote detection of metallic and dielectric artefacts covering underneath the sand surface are performed

using both time and recurrence area estimation data[7, 8]. In[9, 10], GPR concept for landmine spotting and locating individuals in the role of seismic tremor salvage is carried out. Applications of the microwave SFCW method using the SAR technique are proposed for near field image applications [10, 11]. GPR is set up to find cylindrical targets generated with PEC[111, 12] for different soil conditions. The problem of dielectric structure rehabilitation in stratified media [13]. For internal concrete structural inspection, the method of estimation of the propagation time and propagation path model was considered on the basis of the microwave radar method [14]. Data with the corresponding labels were used for training the KNN and the algorithm was subsequently tested and the results obtained showed good accuracy in the classification of objects[15]. WIPL-D models were used to simulate the integrated and diversified/distributed sensors and to check that a substantial improvement was achieved by burying the radiating ring beneath the surface with a received SNR for GPEN [16].

3 Description of Proposed Method

3.1 Microwave Source

A klystron is a vacuum tube that is linear. For super heterodyne radar receivers, these tubes can produce low-power reference signals and generate high-energy transmission waves and drive modern particle accelerometers as amplification devices for microwave and radio frequencies, as shown in **Figure 2**.

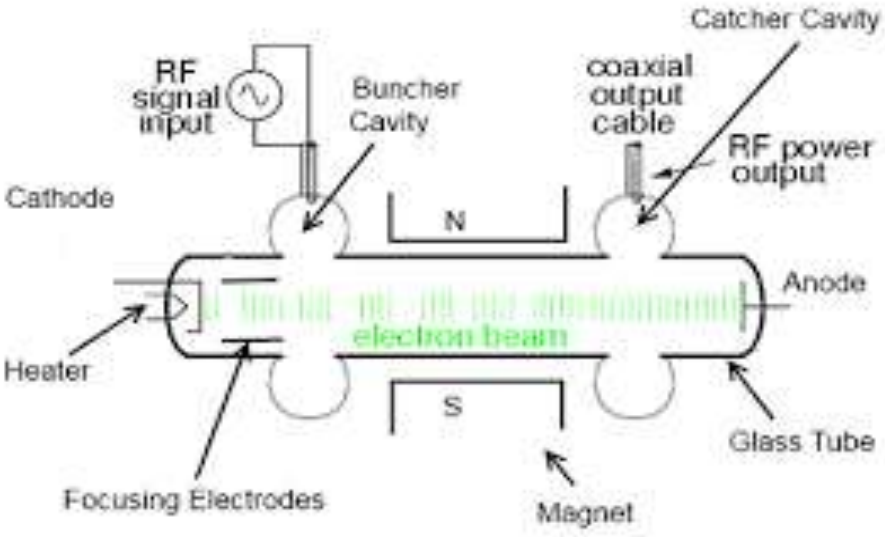

Figure 2 Internal Block of Two Cavity Klystron Amplifier.

3.2 Horn Antenna

Uses for microwave technology include: signal-directed communications, utility and signal power propagation, remote sensor management, pulse-type RADARs, high-rate navigation and, of course,typical consumer goods such as household cooking appliances. In the case of antenna configurations, the approach is to focus a series of microwave signals on a close-in surface, then "slingshot" the total radiated volume back in order to produce an increase in overall gain [17].

The best suited for this application is Horn antenna and is depicted in Figure 3. The radiation characteristics depend on the flare angle, aperture dimension, type of flare, length of the flare. The lowest frequency of operation of a horn is fixed by the cutoff frequency of the waveguide and the neck dimension. The highest frequency gets limited on deterioration in radiation characteristic [18, 19, 20]. The general horn depicted in **Figure 3** has moderate directivity and high gain. The Horn Antenna is used in this work because of its various benefits such as excellent radiating power, low cross polar and side lobes. This ensures that maximum power is coupled to the ground [21, 22].

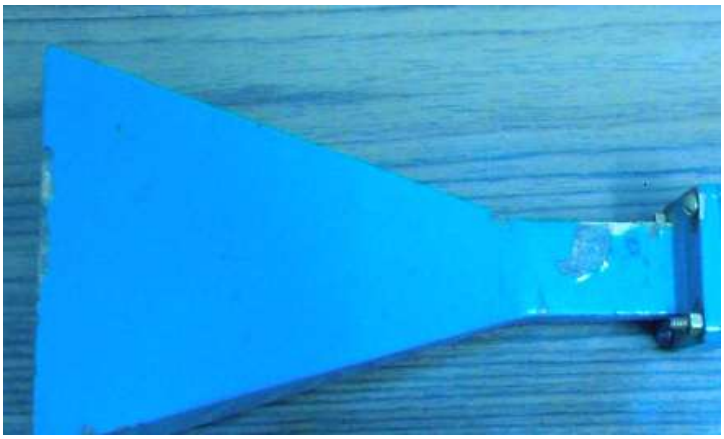

Figure 3 Top View of X Band Horn Antenna used

4 Data Processing Algorithms and Methology

1. A Search for the depth of discontinuity to be found
2. B-scan To locate the discontinuity along a certain length.

4.1 A-scan Flowchart

For the A scan algorithm the steps that are to be followed are depicted in figure 4.

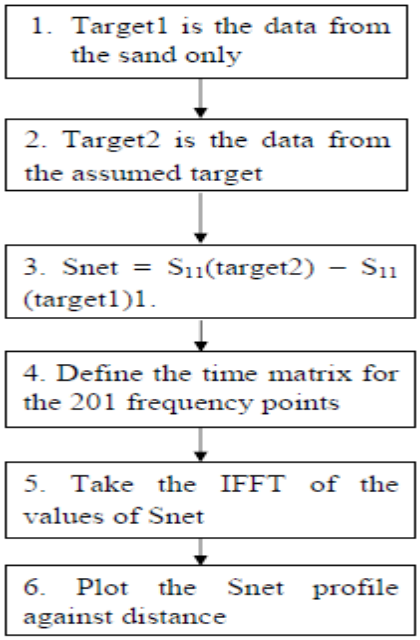

Figure 4 Flowchart of A scan

4.2 A scan Steps

Step 1: Target1 is the frequency domain which includes information about the sand pit's frequency response without any entity buried in it The data for the context sand is called target1.
Step 2; The info in the sand pit for the covered object called target2 and it is the sand pit's original signal information for the unique object buried in it at the place where the detection is being carried out.
Step 3: In the form of S11, the reflection values represent details about the real and imaginary components of the frequency response. The sand pit background information is extracted by subtracting the actual and imaginary parts of the S11 from the background from the S11 values of the buried target.
Step 4: The data for the frequency domain is 201 points. For the conversion of this frequency domain data to the time domain, a time matrix with 201 points must be described.

4.3 B-Scan algorithm

The flow of steps that are to be followed for B scan method are depicted below,

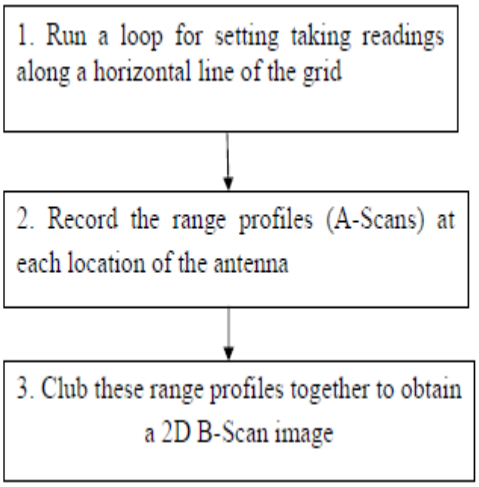

Figure 4 Flowchart of B scan

4.4 B-scan Steps

Step 1: After every reading, the antenna location is altered and the antenna is moved to next pixel location on the observations. Each level is separated 5 cm from the preceding one there are 21 positions in total.
Step 2: Spatial frequency info both for the existence and absence of the target is measured at each of these locations. At all 21 points, these data give the A-Scans
Step 3: For the implementation of a B Scan that senses the particle and provides its one spatial size, all the A-Scans are smacked along the element for evaluation.

Figure 5 depicts the experimental setup used for the proposed model for different scan methods.
Figure 6 depicts three targets buried in the sand pit.

. **Figure 5** Setup for Buried Object Detection

Figure 6 Image of the Cavity, Metal Sheet and Water Bottle Buried In Sand

Table 1 Depicts the Dimensions of the Targets Size and Dielectric Constant of the Targets Buried

Target type	Target size	Dielectric Constant
Air cavity	30 cm by 18cm by 18 cm	1
Metal cavity	25cm by 25cm	∞
Water bottle	30cm, diameter 10cm	80

5 Implementation, Results and Discussion

5.1 A-scan

Data obtained is in the frequency domain that is translated using IFFT to the time domain. As signal intensity verses time delay, the time domain signal is plotted. Highs collected in the plot are checked for where reflections occur and the position of discontinuity is obtained. The reflections of the antenna and soil by context subtraction methods, they are further reported and ignored.

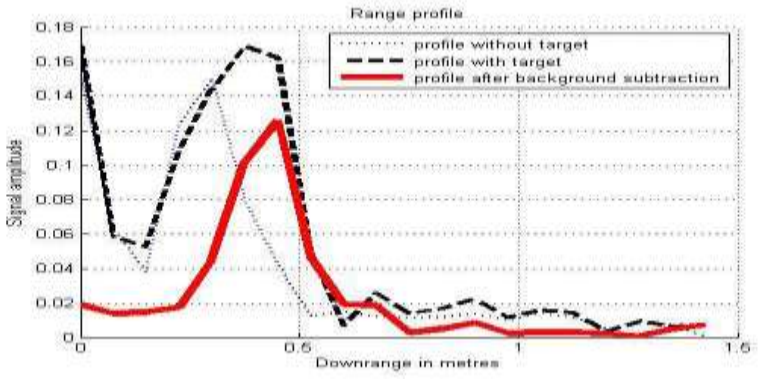

Figure 7 A Scan of Metal Buried 5 cm Below Surface

Figure 7 depicts A – Scan of a metal sheet buried 5 cm. Figure 7 depicts 3 plots. The 1st plot (dotted) is spatial domain when is no target. The 2nd plot(dashed) is range profile when object is buried. The third plot range profile shows the plot when the background data with no target is subtracted from the data with target. This results in a very prominent peak only at the location of the target.

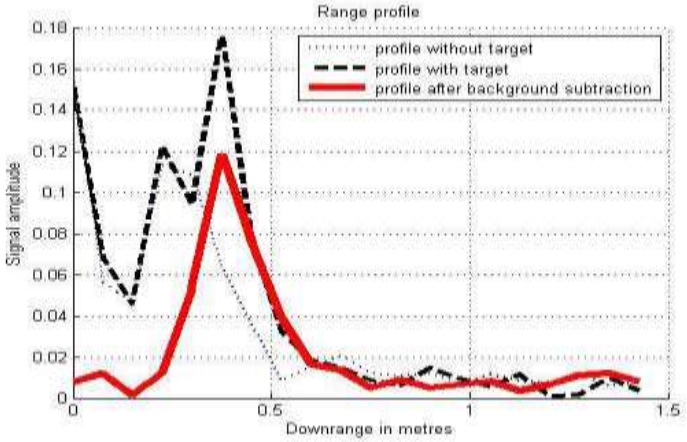

Figure 8 A – Scan of Metal Buried 10 cm Below Surface

Figure 8 depicts A – Scan of metal buried 10 cm below surface. While Figure 8 is the A – Scan of metal buried 15 cm below surface. The A-Scan includes data upon on position of the object and is known as the level of identification.

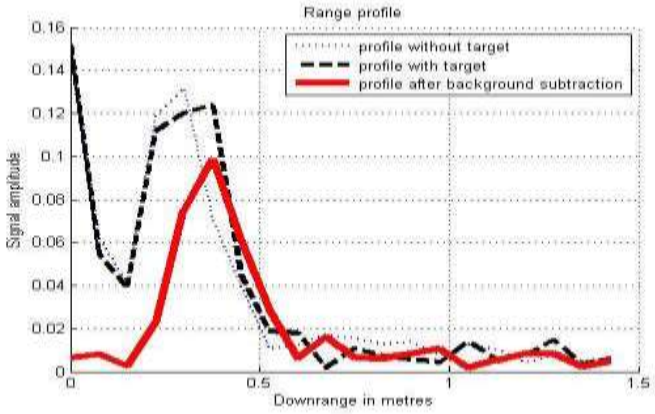

Figure 9 A – Scan of metal buried 15 cm below surface

Figure 7-9 depicts the A-scan method. The solid line indicates subtracted peaks of buried metal used at 15cm has slightly lesser amplitude as compared to the case when sheet was buried 10cm and 5cm below the sand surface.

5.2 A Scan Results – Cavity

Figure 10, 11, 12 depicts cavity buried at 5cm, 10cm, 15cm.

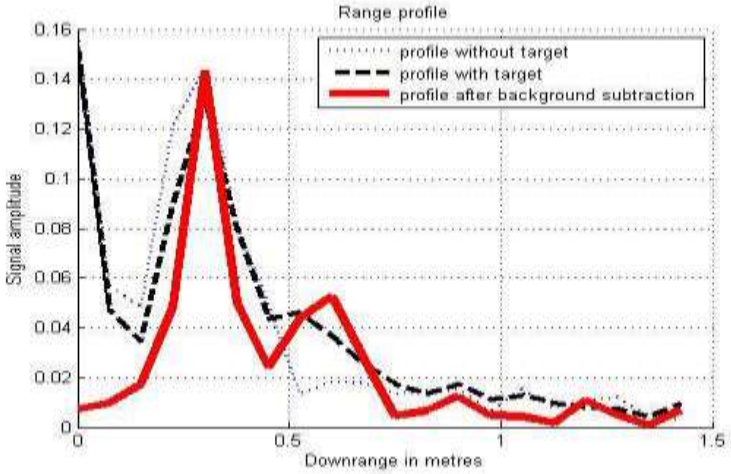

Figure 9 A – Scan of Cavitul Buried 5 cm Below Surface

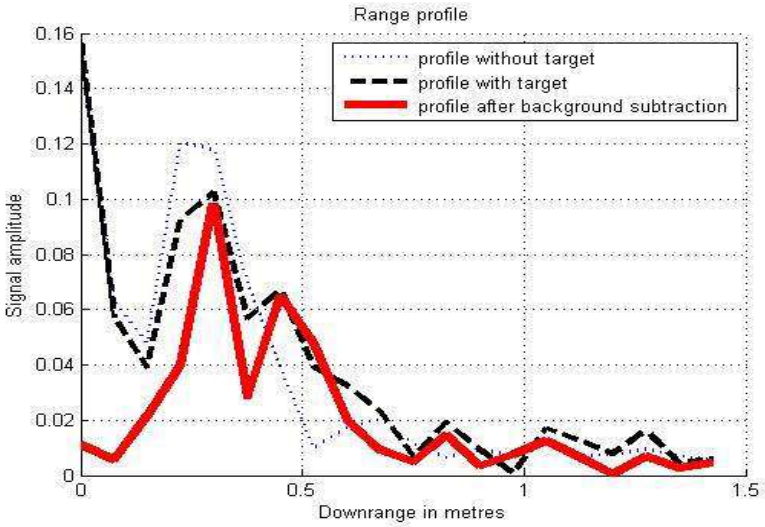

Figure 10 A – Scan of Cavitul Buried 10 cm Below Surface

An interesting aspect in Figure 9, 10 is to note that there are two strong peaks in both the profiles with target and profile after background subtraction. The first peak is the point where the sand-air interface starts. The cavity is 20 cm in depth. Hence there is a second peak where the waves cross the air-sand interface.

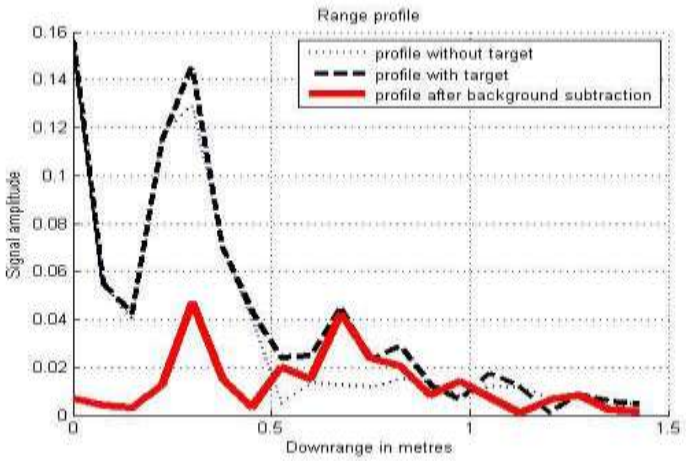

Figure 11 A – Scan of Cavitul Buried 15 cm Below Surface

It is noted that figure 9, 10 and 11 that as the depth of investigation is increased the reflection amplitudes become weaker and weaker. Also the difference in the two peaks becomes lesser in 10 and 15 cm as compared to that at the depth of 5 cm.

5.3 A Scan Results – Water Bottle

Figures 12 -14 show the result obtained after A – Scan detection is used to locate the presence of a water bottle buried 5 cm , 10 cm and 15 cm below the sand surface. It should be noted that the detection of water bottle should theoretically be easier than that of the cavity because it has a much higher dielectric constant than that of the air cavity. But the experiments and the A Scans of the buried cavity and water bottle show that this is not the obtained result.

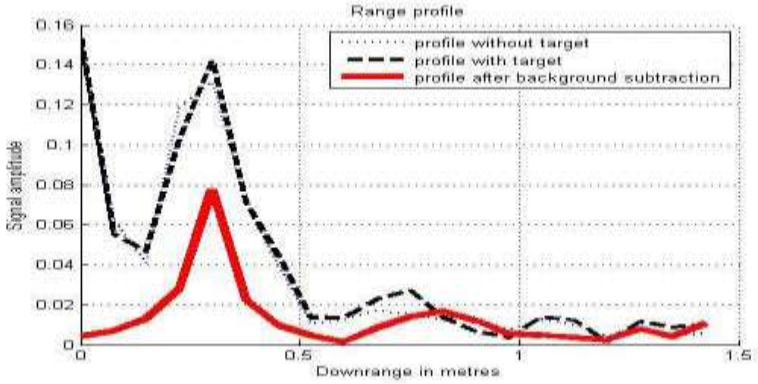

Figure 12 A – Scan of Water Buried 5 cm Below Sand Surface

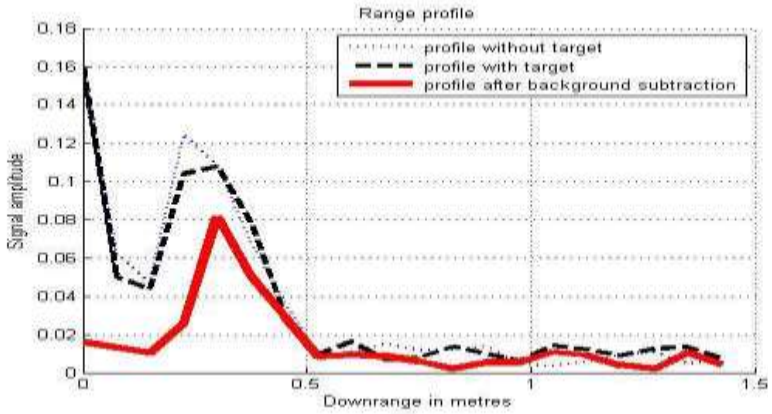

Figure 13 A – Scan of Water Buried 10 cm Below Sand Surface

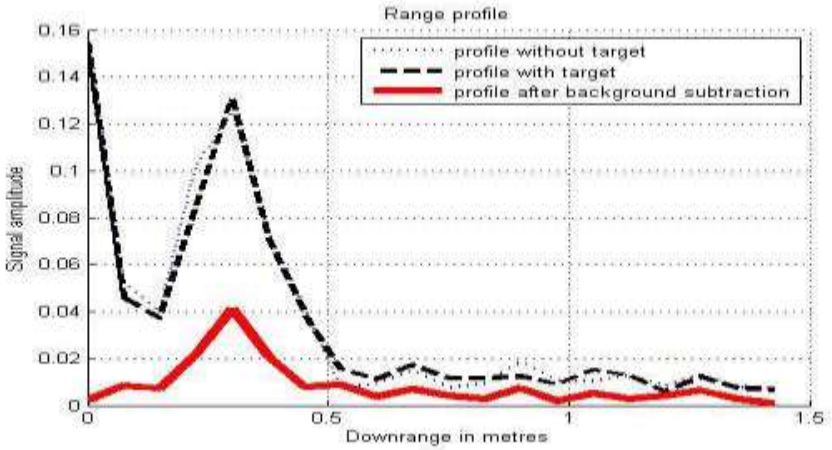

Figure 14 A – Scan of Water Buried 15 cm Below Sand Surface

Reflection amplitudes are found to be lower than in the case of an air cavity. The gap between the peak is also at the depth of 15 cm owing to the combination of the water bottle and that is not relevant level of noise components and hence A-Scan identification fails here, requiring B and C scans for proper imaging.

5.4 B Scan Imaging

5.4.1 Raw B Scan Result

A-Scans are merged through an axis of the sand pit for B Scan imaging, leading in a 2D image being created. This leads in an even more realistic

overview of the studied subsurface. With Imaging, the image is created using the horizontal direction, and the vertical distance. The B scan image of the cavity buried is depicted in figure 15.

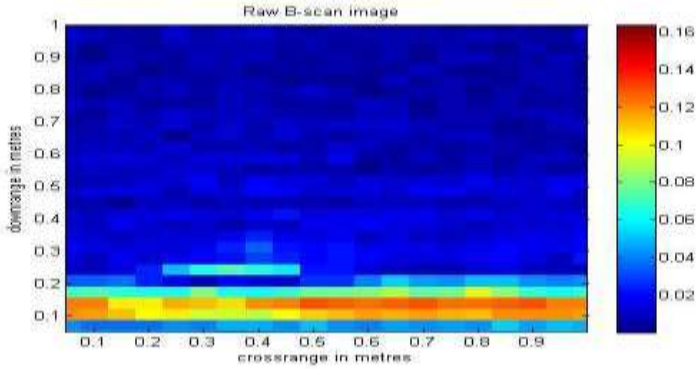

Figure 15 B Scan Image of Cavity Buried 20 cm below the Antenna

Clutter removal using singular value decomposition (SVD) in B scan is employed on the above image and the resultant is depicted in figure 16.

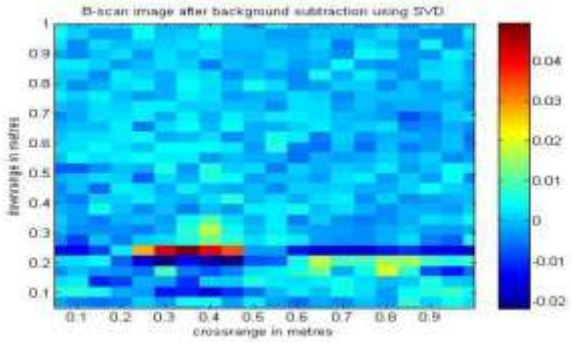

Figure 16 B Scan Image of Cavity Buried 20 cm below the Antenna

After SVD clutter removal, it is found from B Scan image that now the effects of the antenna, sand as well as other factors have decreased a lot and also the image shows clearly the place and one-dimensional scale of the buried cavity.

5.5 Application of Column Filtering and Interpolation on B Scan

After SVD clutter reduction, the B Scan image obtained is found to have steep transitions from one pixel to the other. It can be noted that at one time the antenna would illuminate more than one pixel of the image and hence there would be a filtering feature requirement that could account for these effects

and make the transitions smooth. Therefore the Column Filtering principle and interpolation is employed to improve imaging.

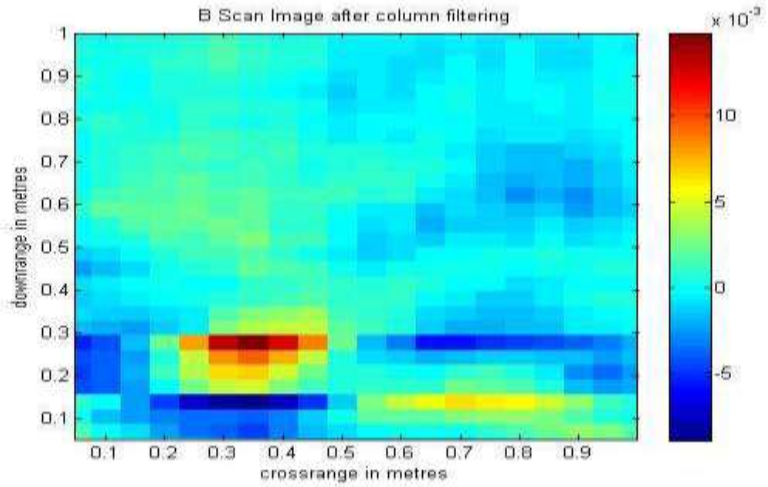

Figure 17 B Scan Image of Cavity at Depth of 20 cm below Antenna after Column Filtering

After SVD, mean and standard deviation based thresholding and Back – Projection Data on Raw B Scan Image is performed and the results are depicted in figure 18 and figure 19.

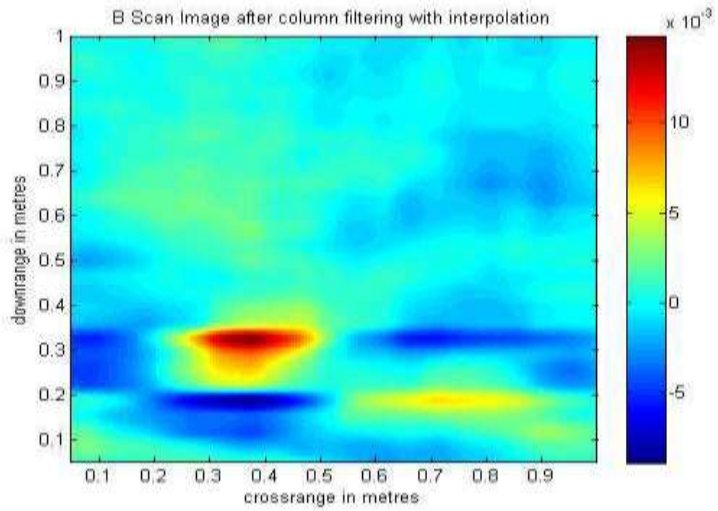

Figure 18 B Scan Image of Cavity at Depth of 20 cm below Antenna After Interpolation

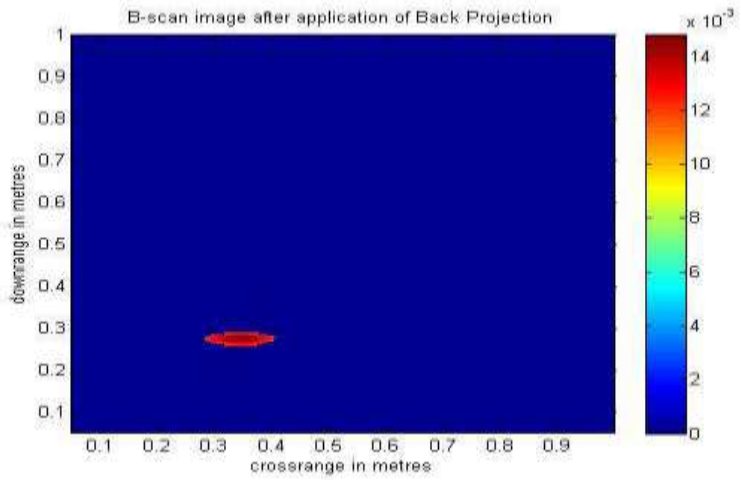

Figure 19 B Scan Image of Cavity Buried 20 cm below Antenna after Back-Projection

After all the processing tools, clutter reduction, column filtering, interpolation and thresholding have been plotted, the final image shows the B Scan of the cavity buried in the subsurface and all the background noise pixels removed.

6 Conclusion and Future Scope

The imaging and detection of the different targets buried at depths from 5 cm to 15 cm was successfully performed and the moisture content increased. A metal board, an air cavity and a water bottle were the objects successfully observed, imaged and marked. Via recognition processes such as A Scan, B Scan, clutter elimination using singular value decomposition, column filtering, interpolation and thresholding, the imaging resulted in detection. The detection of metal was found to be the easiest, followed by the cavity and then the water bottle. For those targets whose dielectric coefficient is much higher than that of the sand medium, the imaging and detection was simpler, since in these cases the reflections are much stronger. The results illustrate that the reflections become weaker at rising depths, the strongest being at 5 cm and 15 cm at the weakest. The experimental results showed that the imaging and identification of buried objects is easier with increasing humidity levels for smaller depths compared to the resolution, whereas the opposite effect is seen for objects buried deeper and thus in with increasing humidity levels, detection and imaging are difficult in these situations.

The algorithm of identification used in the work only works when prior knowledge about the masks of the metal, cavity and water and their dielectric behaviour is available. An improvement in the algorithm may be such that

these masks are not needed, nor is it possible to know about their dielectric behaviour, and it is still possible to identify them successfully. It is also found that due to the reflections in non-normal directions, the water bottle being curved in nature fails proper detection in A Scan. An enhancement in the work may be a methodology that can accurately distinguish curved surfaces.

References

[1]S. Dinç., et al., "Detection and Microwave Imaging of Conducting Objects Buried Very Closely to the Air-Soil Boundary", International Conference on Electromagnetics in Advanced Applications (ICEAA), 2019.

[2]P. Upender, P. A. Harsha Vardhini, "Design of GPR for buried object detection using UWB antenna", International Journal of Engineering and Advanced Technology (IJEAT) IJEAT, Vol. 9, no. 1, pp. 5419-5423, 2019.

[3]W. Susek., M. Knioła., B. Stec., "Buried objects detection using noise radar", 22nd International Microwave and Radar Conference (MIKON), 2018.

[4]P. Upender., "Soil moisture estimation with PALSAR data near Roorkee region", National Conference on Recent Advances in Electronics & Computer Engineering (RAECE), 2015.

[5]P. A. H. Vardhini., N. Koteswaramma., "Patch antenna design with FR-4 Epoxy substrate formultiband wireless communications using CST Microwave studio", International Conference on Electrical Electronics and Optimization Techniques (ICEEOT), 2016.

[6]P. Upender and P. A. Harsha Vardhini, "Design Analysis of Rectangular and Circular Microstrip Patch Antenna with coaxial feed at S-Band for wireless applications", Fourth International Conference on I-SMAC (IoT in Social, Mobile, Analytics and Cloud) (I-SMAC), 2020.

[7]G. Govind., A. Verma., M. J. Akhtar., "Experimental Investigations on Microwave Radar Imaging of Buried Objects", IEEE MTT-S International Microwave and RF Conference (IMaRC), 2018.

[8]S. Dinç., et al., "Detection and Microwave Imaging of Conducting Objects Buried Very Closely to the Air-Soil Boundary", International Conference on Electromagnetics in Advanced Applications (ICEAA), 2019.

[9]S. Paul., R. Chugh., M. J. Akhtar., "Microwave Synthetic Aperture Radar Imaging Using SFCW System for Buried Object Detection and Security Applications," IEEE MTT-S International Microwave and RF Conference (IMARC), 2019.

[10]M. Dogan., G. Turhan-Sayan , "Investigation of the effects of buried object orientation in subsurface target detection by GPR", IEEE International Symposium on Microwave, Antenna, Propagation, and EMC Technologies (MAPE), 2017.

[11]C. Estatico., A. Fedeli., M. Pastorino., A. Randazzo., "Microwave Imaging in Stratified Media: A Multifrequency Inverse-Scattering Approach", 13th European Conference on Antennas and Propagation (EuCAP), 2019.

[12]M. Kubo., M. Okamoto., J. Takayama., "Non-destructive inspection of buried object in concrete structures based on improved propagation path model using microwave radar", 56th Annual Conference of the Society of Instrument and Control Engineers of Japan (SICE), , 2017.

[13]M. Elsaadouny., J. Barowski., I. Rolfes, "Humanitarian Microwave Imaging Enhancement and Classification of Shallowly Buried Objects", IEEE 10th Annual Information Technology, Electronics and Mobile Communication Conference (IEMCON), 2019,.

[14]J. Norgard., R. Musselman., A. Drozd., "Three-dimensional Microwave Tomography: Waveform diversity and distributed sensors for detecting and imaging buried objects with suppressed electromagnetic interference", Asia-Pacific Symposium on Electromagnetic Compatibility and 19th International Zurich Symposium on Electromagnetic Compatibility, 2008.

[15]Jaume, Anguera., Aurora, Andújar., Jeevani, Jayasinghe., " High-Directivity Microstrip Patch Antennas Based on TModd-0 Modes", IEEE Antennas and Wireless Propagation Letters, Vol.19, no. 1, pp.39-43, 2020.

[16]P. Upender., K.R.Anudeep, Laxmikanth., “Shallow metal object Detection at X-Band using ANN and Image analysis Techniques”, IOSR Journal of Electronics and Communication Engineering (IOSR-JECE), Vol.11, no.6, pp. 46-52, 2016.

[17]Balanis CA, “Analysis and Design Antenna Theory,” 2nd ed., J. Peters, John Wiley and Sons, pp. 28-30.

[18]Patri, Upender., P. A. Harsha, Vardhini., “Developing a model to measure the depth metallic landmine with microwave X-band frequency”, International Journal of Developments in Technology and Science, Vol. 1, no.02, 2020.

[19]N. Koteswaramma., P.A. Harsha, Vardhini., K. Murali Chandra Babu., "Realization of Minkowski Fractal Antenna for Multiband Wireless Communication", International Journal of Engineering and Advanced Technology (IJEAT), Vol.9, no.1, pp.5415-5418, 2019.

[20]Salam, Al-Juboori., Xavier Fernando., ‘Multiantenna Spectrum Sensing Over Correlated Nakagami-m Channels with MRC and EGC Diversity Receptions”, IEEE Trans. on Vehicular Tech., Vol.67, no.3, pp.2155-2164, 2018.

[21]P. Upender., G. N. Reddy., G. Santoshini., "Arduino based Accident Prevention System with Eye Twitch and Alcohol sensor," 12th International Conference on Computational Intelligence and Communication Networks (CICN), 2020.

[22]N.Koteswaramma, P.A.Harsha Vardhini, M.Sai Lakshmi, "Fractal Antenna Design Process for Multiband Frequencies", International Journal of Research in Electronics and Computer Engineering (IJRECE), , Vol.7, no. 1, pp. 2468-2472, 2019.

Biographies

Patri Upender, Research Scholar, Dept. of Electronics and Communication Engineering, Sri Satya Sai University of Technology & Medical Sciences, Sehore, Bhopal-Indore Road, MadhyaPradesh, India.

Anil Kumar, Research Guide, Dept. of Electronics and Communication Engineering, Sri Satya Sai University of Technology & Medical Sciences, Sehore, Bhopal Indore Road,Madhya Pradesh, India.